

Perovskite Solar Cells Based on Oligotriarylamine Hexaarylbenzene as Hole-Transporting Materials

Mona Shasti,^{†,§,#} Sebastian F. Völker,^{‡,#} Silvia Collavini,[‡] Silvia Valero,[‡] Fernando Ruipérez,^{‡,||} Abdollah Mortezaali,[§] Shaik. M. Zakeeruddin,^{||} M. Grätzel,^{*,||,||} A. Hagfeldt,^{*,†} and Juan Luis Delgado^{*,‡,||,||}

[†]Laboratory for Photonics and Interfaces, Institute of Chemical Sciences and Engineering, École Polytechnique Fédérale de Lausanne, CH-1015 Lausanne, Switzerland

[‡]POLYMAT, University of the Basque Country UPV/EHU. Avenida de Tolosa 72, 20018 Donostia-San Sebastián, Spain

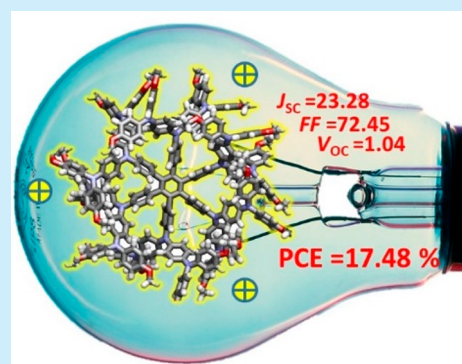
[§]Department of Physics, Alzahra University, Tehran 1993893973, Iran

^{||}Laboratory for Photonics and Interfaces, Institute of Chemical Sciences and Engineering, École Polytechnique Fédérale de Lausanne, CH-1015 Lausanne, Switzerland

^{||}Ikerbasque, Basque Foundation for Science, 48013 Bilbao, Spain

Supporting Information

ABSTRACT: A cobalt-catalyzed cyclotrimerization of bis(aryl)alkyne is used as an innovative tool to obtain hole-transport materials (HTMs). The novel HTM containing six units of oligotriarylamine (**HAB1**), characterized by UV–vis, cyclic voltammetry, DFT, and thermogravimetric analysis, confirms its suitability as an efficient HTM in PSCs. A PCE of 17.5% was obtained in **HAB1**-containing PSCs, a performance comparable to that obtained with spiro-OMeTAD and with slightly better thermal stability.



Perovskite solar cells (PSCs) have revolutionized the scientific community in recent years, thanks to their outstanding ability to transform sunlight into electricity.¹ In the search for new materials that could increase the stability and the efficiency of these cells, organic molecules have played an important role as electron-transport materials (ETMs), hole-transport materials (HTMs), or additives within the perovskite layer.²

The most successful organic materials employed in PSCs so far, namely spiro-OMeTAD as HTM and fullerenes as ETMs, display a globular or semiglobular shape, which might be one of the reasons for their good performance, due to facilitated charge injection and extraction even with a nonoptimized film morphology.² Apart from the aforementioned materials, further three-dimensional HTMs have already proven to work very efficiently in combination with perovskites.³ The big majority of HTMs reported in the literature are based on triarylamines (TAAs) or TAA derivatives,⁴ owing to the primary properties of TAAs to transport holes and block electrons, which seem to be vital for suitable organic HTMs design.

Cyclotrimerization of alkynes has been used as an elegant and efficient tool to build innovative molecules to investigate intramolecular charge transport and organic electronics or to

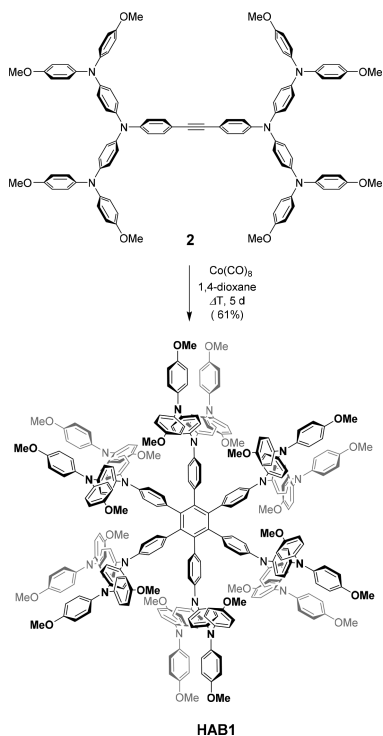
construct dendritic-shaped fullerenes, among others.⁵ Considering all these concepts, we have designed a novel HTM structure through cobalt-catalyzed cyclotrimerization of alkynes to afford a hexaarylbenzene core endowed with six oligotriarylamine fragments (**HAB1**, Scheme 1).

The novel derivative **HAB1** was synthesized according to a multistep protocol displayed in Scheme S1. Compound **2** was obtained through a palladium-catalyzed amination reaction between amine **1** and 1,2-bis(4-bromophenyl)ethylene using Pd(dba)₂ and PtBu₃ as the catalytic system. This palladium-catalyzed amination reaction afforded **2** as an orange solid in a high 89% yield.

Cobalt-catalyzed cyclotrimerization of bis(aryl)alkyne oligotriarylamine (**2**) afforded the hexaarylbenzene core endowed with six oligotriarylamine fragments (**HAB1**, Scheme 1) with a 61% yield. The novel material and intermediates were fully characterized by nuclear magnetic resonance (NMR) and high-resolution mass spectrometry (HR-MS), confirming the chemical identity of the materials as well as its high purity. Furthermore, cyclic voltammetry, UV–vis absorption spec-

Received: March 20, 2019

Scheme 1. Synthesis of the Novel Derivative HAB1



troscopy, and TD-DFT computational studies confirmed the suitability of **HAB1** to act as efficient HTM.

The ^1H NMR spectrum of **HAB1** shows, together with the aromatic protons, the diagnostic singlet at 3.30 ppm, which is assigned to the 24 symmetric methoxy groups, perfectly integrating 72 hydrogen atoms (Figure S3). HRMS analysis of **HAB1** further confirmed the chemical identity and purity of this novel material. MALDI-TOF in positive mode of detection shows a strong peak at m/z 4261.8148 assigned to the molecular ion peak of **HAB1**. This experimental finding agrees with the theoretical molecular ion peak mass of the new material (calculated for $\text{C}_{282}\text{H}_{240}\text{N}_{18}\text{O}_{24}$ m/z 4261.8112, Figure S8).

The absorption spectrum of **HAB1** was recorded in methylene chloride and shows intense absorption bands in the UV region, which are assigned to the six oligotriarylamine fragments.^{6a} These chemical fragments are also linked to the high extinction coefficient displayed by the UV absorption bands of the novel compound. On the contrary, **HAB1** shows nearly no contribution in the visible part of the spectrum, which is a desirable feature of every HTM candidate (Figure S5).

The electrochemical properties of **HAB1** were investigated by means of cyclic voltammetry in methylene chloride as solvent. In the cyclic voltammogram of **HAB1** it is possible to observe the typical three quasi-reversible one-electron oxidation waves of this kind of systems (I–III).⁶ In addition there is a fourth irreversible oxidation wave, which has been previously observed in similar molecules and assigned to the formation of polycationic species (IV).^{6a} In agreement with the literature, we can assign the first oxidation wave (I, $E_{\text{ox}} = 0,02 \text{ V}$) to the removal of one electron from the central TPA moiety, which is closer to the hexaarylbenzene core. Thus, oxidation waves II and III (II, $E_{\text{ox}} = 0,30 \text{ V}$ and III, $E_{\text{ox}} = 0,80 \text{ V}$) correspond to the removal of one electron each from the

4,4-dimethoxydiphenylamine fragments present on the oligotriarylamine moiety.

The HOMO level of **HAB1** was estimated from the half-wave potentials extracted from the cyclic voltammogram shown in Figure 1.⁷ Using the onset on the low energy side of the lowest energy absorption band we obtained the band gap of **HAB1**.

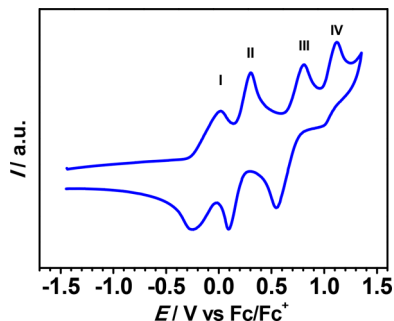


Figure 1. Cyclic voltammogram of **HAB1** in DCM/TBAHFP (0.1 M) vs Fc/Fc^+ at a scanning rate of 250 mV s^{-1} .

With the HOMO energy and the band gap obtained, respectively, from the cyclic voltammogram and the absorption spectroscopy we calculated the LUMO. As it can be seen in Figure 2, **HAB1** not only has good prerequisites to work as an HTM but also serves as electron blocking material to avoid recombination of electrons.

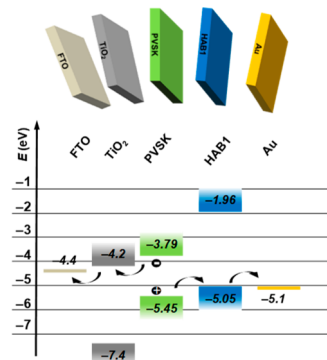


Figure 2. Cell architecture and energy levels of the applied materials in the PSC. The bond lengths between the central benzene carbons and the substituting moieties range between 1.499 and 1.501 Å, with a mean value of 1.500 Å.

Furthermore, as shown through thermogravimetric analysis (TGA), the thermal stability of **HAB1** is higher than that of spiro-OMeTAD (Figure S10). Temperatures corresponding to 2% or 5% weight loss for both compounds were recorded by TGA, and the results indicated a higher thermal stability of **HAB1**. This is indeed a benefit for the preparation of stable perovskite solar cells containing the novel compound. Moreover, we have performed density functional theory calculations (DFT) of **HAB1** with the Gaussian 16 suite of programs.⁸ Structure optimization was performed in the gas phase using the B3LYP functional^{9,10} and the 6-31G(d) basis set.¹¹ The optimized molecular structure of the **HAB1** molecule is displayed in Figure S14. It is clearly appreciable how the six phenyl groups attached to the central benzene are twisted due to the large steric hindrance that the amino groups

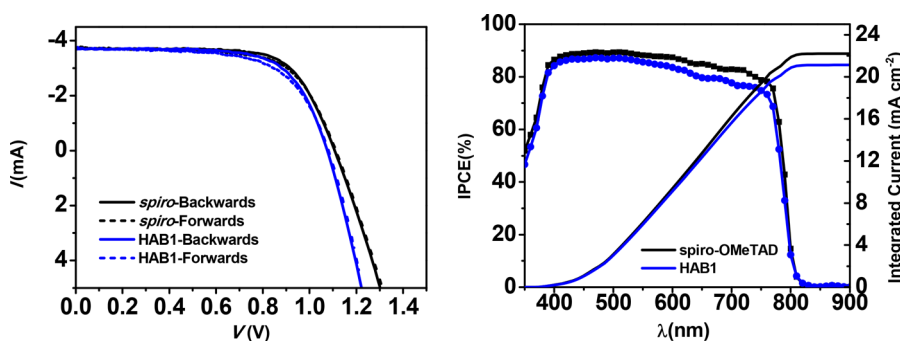


Figure 3. (Left) I - V curves of the best spiro- and **HAB1**-containing devices. For spiro, the obtained PCE was 18.45% (J_{SC} 23.34 mA cm⁻², V_{OC} 1.07 V, FF 74%); for **HAB1**, it was 17.48% (J_{SC} 23.28 mA cm⁻², V_{OC} 1.04 V, FF 72%). (Right) Incident photon-to-current efficiency (IPCE) curves for reference and **HAB1**-containing device.

in *para* position exert. Thus, the dihedral angles between the substituting rings and the central one varies from 73.9° to 67.2°, with a mean value of $\theta = 71.0^\circ$.

To evaluate its behavior as a hole-transport material, **HAB1** was incorporated in regular, mesoporous PSCs. The perovskite composition used for this study is Cs_{0.5}(MA_{0.15}FA_{0.85})_{0.95}Pb(I_{0.85}Br_{0.15}), also known as triple-cation perovskite.¹² The device structure is the following: (FTO)/compact TiO₂/mesoporous TiO₂/Cs_{0.5}(MA_{0.15}FA_{0.85})_{0.95}Pb(I_{0.85}Br_{0.15})/**HAB1**/Au. The detailed fabrication procedure can be found in the SI. As an HTM reference, we chose the widely used 2,2',7,7'-tetrakis(*N,N*-di-4-methoxyphenylamino)-9,9'-spiro-bifluorene (spiro-OMeTAD). These molecules require the addition of small amounts of dopants in order to achieve their maximum performances. These additives, in fact, help to increase the performances of the HTM. A recent work by Qi et al. focuses on two of these dopants, bis-(trifluoromethylsulfonyl)imide lithium salt (LiTFSI) and 4-*tert*-butylpyridine (TBP).¹³ They confirmed the role of LiTFSI in enhancing the conductivity and the kinetics of the oxidation of the HTM. Two different conditions were investigated for the doping of **HAB1**. In both cases, TBP and Li-TFSI were used. When no other additive was used, the **HAB1**-containing devices gave a best power conversion efficiency (PCE) of 16.77%. The addition of tris(2-(1*H*-pyrazol-1-yl)-4-*tert*-butylpyridine)cobalt(III) tri[bis(trifluoromethane)sulfonimide] (FK209) helped in enhancing the best PCE to 17.48%, mostly due to an improvement of the fill factor (FF) from 70 to 72%. It is also worth pointing out that the globular structure displayed by **HAB1** contributes to the formation of high quality films. In this regard a recent report indicates that when OTA based-molecule is flat the devices display low performance, mainly due to low quality of the films.¹⁴

Figure S13 summarizes the statistics of the PV parameters of the studied devices. Both the open-circuit voltage (V_{OC}) and the short-circuit current (J_{SC}) are very similar to those of spiro-OMeTAD, resulting from the comparable HOMO energy levels of the HTMs and indicating similar charge conductivity. The slight improvement obtained with the addition of FK209 is mainly due to the fact that this cobalt compound shifts down **HAB1**'s HOMO level by oxidizing the molecule, thus creating a larger energy gap between Fermi level of TiO₂ and the HOMO level of HTM, leading to higher V_{OC} .¹⁵ By lowering the HOMO level, the difference between valence band of perovskite and HTM is reduced, hence contributing to the easier charge extraction and resulting in PCE enhancement.¹⁶

Backward and forward scans for spiro-OMeTAD and **HAB1**-containing devices are shown in Figure 3. Dark current measurements can be seen in Figure S11. The J - V characteristics and maximum PCE were measured again after 3 and 10 days and summarized in Table S2. PCE in reverse scan for spiro-OMeTAD-based devices decreased 0.51% after 3 days and 0.57% after 10 days. For **HAB1**-based devices, in the backward scan direction PCE decreased 0.56% and 0.57% after 3 and 10 days, respectively, thus indicating that the stability of **HAB1**-containing devices is comparable to that of spiro-reference devices. The integrated current obtained by IPCE measurements shows interesting behavior. This value is increasing from 22.21 and 21.13 mA cm⁻² to 22.27 and 21.51 mA cm⁻² for the control and the new HTM-based devices after 10 days, respectively. It was observed that the improvement of the integrated current is linked to the reduction of the hysteresis (Table S2). IPCE curves for devices 10 days after preparation are shown in Figure 3, where a slightly faster decrease in current for **HAB1** can be noticed. This can be attributed to mismatch in either the interface of **HAB1**-gold or **HAB1**-perovskite layer. Ten days after the preparation of the cells, the maximum power point (MPP) was tracked (Figure S12). The MPP value for both the reference and the **HAB1**-containing devices increases during the aging of the cells, being correlated with the reported reduction of the hysteresis with time (Table S2). To summarize, we have prepared a novel HTM based on a hexaarylbenzene central core endowed with six units of oligotriarylamine (**HAB1**).

This material has been fully characterized by UV-vis, cyclic voltammetry, DFT, and thermogravimetric analysis, and the results confirms its suitability to act as an effective HTM in PSCs. Indeed, when **HAB1** is incorporated in PSCs within the architecture (FTO)/compact TiO₂/mesoporous TiO₂/Cs_{0.5}(MA_{0.15}FA_{0.85})_{0.95}Pb(I_{0.85}Br_{0.15})/**HAB1**/Au a PCE of 17.5% was obtained. The simplicity of the synthetic approach employed for the preparation of **HAB1** makes it a very efficient and low cost method to obtain novel HTMs being able to compete with spiro-OMeTAD. Considering the easy and versatile chemistry employed in this approach, other HT moieties such as porphyrins, phthalocyanines, or modified TPAs can be easily incorporated to tune the HT properties of HABS, thus obtaining improved HABS able to surpass the state of the art PCE in this field.

■ ASSOCIATED CONTENT

Supporting Information

The Supporting Information is available free of charge on the ACS Publications website at DOI: [10.1021/acs.orglett.9b00988](https://doi.org/10.1021/acs.orglett.9b00988).

Experimental methods, supporting characterization figures, perovskite solar cell preparation, and characterization data (PDF)

■ AUTHOR INFORMATION

Corresponding Authors

*E-mail: michael.gratzel@epfl.ch.

*E-mail: anders.hagfeldt@epfl.ch.

*E-mail: juanluis.delgado@polymat.eu.

ORCID

Fernando Ruipérez: 0000-0002-5585-245X

M. Grätzel: 0000-0002-0068-0195

Juan Luis Delgado: 0000-0002-6948-8062

Author Contributions

#M.S. and S.F.V. contributed equally to this work.

Notes

The authors declare no competing financial interest.

■ ACKNOWLEDGMENTS

We are grateful to Ikerbasque, POLYMAT, UPV/EHU (Grupo de Investigación GIU17/054), and Gobierno de España (MINECO CTQ2015-70921). M.G. and S.M.Z. thank the King Abdulaziz City for Science and Technology (KACST) for financial support. S.C. acknowledges the Basque Government for a PREDOC grant. M.S. acknowledges the Ministry of Science, Research and Technology of Iran, for financial support. Technical and human support provided by IZO-SGI, SGIker (UPV/EHU, MICINN, GV/EJ, ERDF, and ESF) is gratefully acknowledged for assistance and generous allocation of computational resources.

■ REFERENCES

- (1) Park, N.-G.; Grätzel, M.; Miyasaka, T.; Zhu, K.; Emery, K. *Nat. Energy* **2016**, *1*, 16152.
- (2) (a) Völker, S. F.; Collavini, S.; Delgado, J. L. *ChemSusChem* **2015**, *8*, 3012–3028. (b) Collavini, S.; Völker, S. F.; Delgado, J. L. *Angew. Chem., Int. Ed.* **2015**, *54*, 9757–9759. (c) Ameen, S.; Rub, M. A.; Kosa, S. A.; Alamry, K. A.; Akhtar, M. S.; Shin, H.-S.; Seo, H.-K.; Asiri, A. M.; Nazeeruddin, M. K. *ChemSusChem* **2016**, *9*, 10–27. (d) Li, H.; Fu, K.; Boix, P. P.; Wong, L. H.; Hagfeldt, A.; Grätzel, M.; Mhaisalkar, S. G.; Grimsdale, A. C. *ChemSusChem* **2014**, *7*, 3420–3425. (e) Pascual, J.; Delgado, J. L.; Tena-Zaera, R. *J. Phys. Chem. Lett.* **2018**, *9*, 2893–2902. (f) Kazim, S.; Nazeeruddin, M. K.; Grätzel, M.; Ahmad, S. *Angew. Chem., Int. Ed.* **2014**, *53*, 2812–2824. (g) Urieta-Mora, J.; Garcia-Benito, L.; Molina-Ontoria, A.; Martín, N. *Chem. Soc. Rev.* **2018**, *47*, 8541–8571.
- (3) (a) Krishna, A.; Sabba, D.; Li, H.; Yin, J.; Boix, P. P.; Soci, C.; Mhaisalkar, S. G.; Grimsdale, A. C. *Chem. Sci.* **2014**, *5*, 2702–2709. (b) Ganesan, P.; Fu, K.; Gao, P.; Raabe, I.; Schenk, K.; Scopelliti, R.; Luo, J.; Wong, L. H.; Grätzel, M.; Nazeeruddin, M. K. *Energy Environ. Sci.* **2015**, *8*, 1986–1991. (c) Li, M.-H.; Hsu, C.-W.; Shen, P.-S.; Cheng, H.-M.; Chi, Y.; Chen, P.; Guo, T.-F. *Chem. Commun.* **2015**, *51*, 15518–15521. (d) Zhang, M.; Wang, G.; Zhao, D.; Huang, C.; Cao, H.; Chen, M. *Chem. Sci.* **2017**, *8*, 7807–7814.
- (4) (a) Vivo, P.; Salunke, J.; Priimagi, A. *Materials* **2017**, *10*, 1087. (b) Wang, J.; Liu, K.; Ma, L.; Zhan, X. *Chem. Rev.* **2016**, *116*, 14675–14725. (c) Agarwala, P.; Kabra, D. *J. Mater. Chem. A* **2017**, *5*, 1348–1373.
- (5) (a) Lambert, C.; Nöll, G. *Chem. - Eur. J.* **2002**, *8*, 3467–3477. (b) Lambert, C.; Nöll, G. *Angew. Chem., Int. Ed.* **1998**, *37*, 2107–2110. (c) Hirao, Y.; Ishizaki, H.; Ito, A.; Kato, T.; Tanaka, K. *Eur. J. Org. Chem.* **2007**, *2007*, 186–190. (d) Rosokha, S. V.; Neretin, I. S.; Sun, D.; Kochi, J. K. *J. Am. Chem. Soc.* **2006**, *128*, 9394–9407. (e) Wu, I. Y.; Lin, J. T.; Tao, Y. T.; Balasubramaniam, E. *Adv. Mater.* **2000**, *12*, 668–669. (f) Yoshida, K.; Morimoto, I.; Mitsudo, K.; Tanaka, H. *Tetrahedron Lett.* **2008**, *49*, 2363–2365. (g) Hahn, U.; Maisonhaute, E.; Amatore, C.; Nierengarten, J.-F. *Angew. Chem., Int. Ed.* **2007**, *46*, 951–954. (h) Kou, C.; Feng, S.; Li, H.; Li, W.; Li, D.; Meng, Q.; Bo, Z. *ACS Appl. Mater. Interfaces* **2017**, *9*, 43855–43860.
- (6) (a) Hirao, Y.; Ito, A.; Tanaka, K. *J. Phys. Chem. A* **2007**, *111*, 2951–2956. (b) Bonn, A. G.; Wenger, O. S. *Phys. Chem. Chem. Phys.* **2015**, *17*, 24001–24010. (c) Bozic-Weber, B.; Brauchli, S. Y.; Constable, E. C.; Furer, S. O.; Housecroft, C. E.; Wright, I. A. *Phys. Chem. Chem. Phys.* **2013**, *15*, 4500–4504.
- (7) The details concerning HOMO estimation of HAB 1 can be found in the SI.
- (8) *Gaussian 16*, Revision B.01: Frisch, M. J.; Trucks, G. W.; Schlegel, H. B.; Scuseria, G. E.; Robb, M. A.; Cheeseman, J. R.; Scalmani, G.; Barone, V.; Petersson, G. A.; Nakatsuji, H.; Li, X.; Caricato, M.; Marenich, A. V.; Bloino, J.; Janesko, B. G.; Gomperts, R.; Mennucci, B.; Hratchian, H. P.; Ortiz, J. V.; Izmaylov, A. F.; Sonnenberg, J. L.; Williams-Young, D.; Ding, F.; Lipparini, F.; Egidi, F.; Goings, J.; Peng, B.; Petrone, A.; Henderson, T.; Ranasinghe, D.; Zakrzewski, V. G.; Gao, J.; Rega, N.; Zheng, G.; Liang, W.; Hada, M.; Ehara, M.; Toyota, K.; Fukuda, R.; Hasegawa, J.; Ishida, M.; Nakajima, T.; Honda, Y.; Kitao, O.; Nakai, H.; Vreven, T.; Throssell, K.; Montgomery, J. A., Jr.; Peralta, J. E.; Ogliaro, F.; Bearpark, M. J.; Heyd, J. J.; Brothers, E. N.; Kudin, K. N.; Staroverov, V. N.; Keith, T. A.; Kobayashi, R.; Normand, J.; Raghavachari, K.; Rendell, A. P.; Burant, J. C.; Iyengar, S. S.; Tomasi, J.; Cossi, M.; Millam, J. M.; Klene, M.; Adamo, C.; Cammi, R.; Ochterski, J. W.; Martin, R. L.; Morokuma, K.; Farkas, O.; Foresman, J. B.; Fox, D. J. *Gaussian, Inc.*, Wallingford, CT, 2016.
- (9) Lee, C.; Yang, W.; Parr, R. G. *Phys. Rev. B: Condens. Matter Mater. Phys.* **1988**, *37*, 785–789.
- (10) Becke, A. D. *J. Chem. Phys.* **1993**, *98*, 5648–5652.
- (11) Hehre, W. J.; Ditchfield, R.; Pople, J. A. *J. Chem. Phys.* **1972**, *56*, 2257–2261.
- (12) Saliba, M.; Matsui, T.; Seo, J. Y.; Domanski, K.; Correa-Baena, J. P.; Nazeeruddin, M. K.; Zakeeruddin, S. M.; Tress, W.; Abate, A.; Hagfeldt, A.; Grätzel, M. *Energy Environ. Sci.* **2016**, *9*, 1989–1997.
- (13) Juarez-Perez, E. J.; Leyden, M. R.; Wang, S.; Ono, L. K.; Hawash, Z.; Qi, Y. *Chem. Mater.* **2016**, *28*, 5702–5709.
- (14) Völker, S. F.; Vallés-Pelarda, M.; Pascual, J.; Collavini, S.; Ruipérez, F.; Zuccatti, E.; Hueso, L. E.; Tena-Zaera, R.; Mora-Seró, I.; Delgado, J. L. *Chem. - Eur. J.* **2018**, *24*, 8524–8529.
- (15) Xi, H.; Tang, S.; Ma, X.; Chang, J.; Chen, D.; Lin, Z.; Zhong, P.; Wang, H.; Zhang, C. *ACS Omega* **2017**, *2*, 326–336.
- (16) Sanchez, R. S.; Mas-Marza, E. *Sol. Energy Mater. Sol. Cells* **2016**, *158*, 189–194.